
Mathematical modelling of pressure distribution along the die of a biomass briquetting machine

Joseph Ifeolu Orisaleye* and
Sunday Joshua Ojolo

Department of Mechanical Engineering,
University of Lagos,
Akoka, Nigeria
Email: jorisaleye@unilag.edu.ng
Email: sojolo@unilag.edu.ng
*Corresponding author

Abstract: The screw extruder briquetting die is critical to determining the quality of biomass briquettes. In this study, mathematical models were developed to study pressure distribution along the briquetting die using the hot extrusion scheme and assuming a plug flow. Parametric analysis to determine the effects of design variables on die pressure distribution was carried out by simulation using developed mathematical models. Results showed that pressure along the die entry decreases rapidly with high yield strength of compacted biomass and with increased friction coefficient at the briquetting die interface. As friction coefficient at the die interface increases, there is rapid decrease in pressure along the length of the die. Parameters resulting in rapid pressure decrease along the briquetting die length would result in increased die pressure at the end of the screw extruder. The developed mathematical models and the results obtained could significantly contribute to design of briquetting dies.

Keywords: biomass densification; solid fuel; screw extruder briquetting machine; pressure distribution; die pressure; mathematical model; plug flow; parametric analysis; design engineering.

Reference to this paper should be made as follows: Orisaleye, J.I. and Ojolo, S.J. (2019) 'Mathematical modelling of pressure distribution along the die of a biomass briquetting machine', *Int. J. Design Engineering*, Vol. 9, No. 1, pp.36–50.

Biographical notes: Joseph Ifeolu Orisaleye obtained a Bachelor of Technology in Mechanical Engineering from Ladoko Akintola University of Technology, Ogbomoso, Nigeria and a Master of Science in Mechanical Engineering from University of Lagos, Akoka, Nigeria with specialisation in Design and Production Engineering. He pursued a Doctor of Philosophy in Mechanical Engineering. At present, he is a Lecturer at the Department of Mechanical Engineering, University of Lagos, Nigeria. His research interests are in renewable energy systems and machine design. He is a member of the Nigerian Society of Engineers and Nigerian Institution of Mechanical Engineering. He is also a Registered Engineer.

Sunday Joshua Ojolo holds a PhD in Farm Power and Machinery from University of Ibadan in 2004. His area of specialisation is in machinery development, manufacturing engineering and energy systems. At present, he is an Associate Professor of Machine Design and Manufacturing Engineering in University of Lagos since 2016. He has published over 70 research papers in

reputable journals. He is a member of America Society of Mechanical Engineers, Nigerian Society of Engineers; a Fellow at Nigerian Institution of Mechanical Engineering; COREN Registered Engineer. He is on the editorial board of five reputable international journals. He is a consultant to many industries.

1 Introduction

Regional and global studies have shown that biomass energy has a huge potential for the replacement of the largely used conventional energy sources (Maurya et al., 2018; Ojolo et al., 2012a; Smeets et al., 2005). However, raw biomass has inherent poor properties which make transport and direct usage problematic. Raw biomass is hygroscopic, has high moisture content, low bulk density and poor combustion properties (Manickam and Suresh, 2011). The utilisation of raw biomass in combustion and gasification facilities can be made more efficient by densification of raw biomass into solid fuels (Ojolo and Orisaleye, 2010; Ojolo et al., 2012b; Kumararaja, 2009).

Existing biomass densification technologies for the production of solid fuels include briquetting, pelleting, cubing and agglomeration. The briquetting technologies include the mechanical piston press, hydraulic piston press and screw extruder. The screw extruder briquetting machines have been shown to produce high quality solid fuel which is suitable for use in both gasification and combustion systems (Tumuluru et al., 2010). However, the trial-and-error method is often used when technical and design parameters in the compaction process are set (Jarošová and Kureková, 2013; Hardman, 2001). This has resulted in several operational problems for the screw extruder briquetting machine which include rapid screw wear and high power requirement (Tumuluru et al., 2010). This has necessitated the development of theoretical approaches for the study and the design of the screw extruder briquetting machine.

Some work has been done in the development of mathematical models for the study of the screw extruder of the biomass briquetting machine. Ojolo et al. (2015) presented a mathematical model for the study of pressure developed in a tapered screw extruder biomass briquetting. The study investigated the effects of geometrical and operational parameters on pressure in the screw extruder. Similar studies had been carried out by Matúš et al. (2011) for the force analysis to determine the pressure developed in the extruder. Orisaleye and Ojolo (2019) developed a mathematical model used to carryout parametric analysis of design parameters of straight screw extruders for solids compaction. Zhong (1991) investigated the compaction process in a tapered screw extruder using numerical models and experimental approaches. Orisaleye et al. (2019) studied the screw wear of the screw extruder briquetting machine by the development of mathematical models.

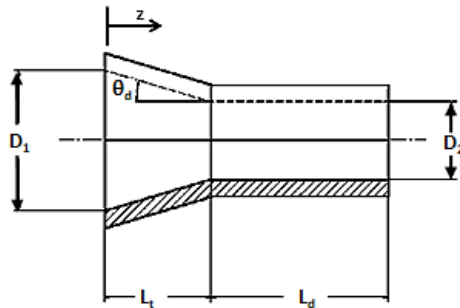
The briquetting die is at the end of the screw extruder and gives the briquette the final form. Križan et al. (2009) presented a model for the determination of counter-pressure in the pressing chamber during compaction. Križan et al. (2012) classified pressing chambers of briquetting machines into closed pressing chamber and open pressing chamber systems. For the open pressing chamber, which is suitable for the die of the screw extruder briquetting machine, counter pressure is created by friction forces from compacted material within the pressing chamber. Križan et al. (2010) and Kováčová et al.

(2014) also presented mathematical models to investigate the effect of the conical chamber on briquetting pressure based on friction at the die interface but did not consider the inherent properties of the compacted materials. Behravesh et al. (2010) carried out a theoretical study to predict the die pressure in wood-plastic composites extrusion with experimental verification. The theoretical study explored non-Newtonian flow and the hot extrusion scheme and it was noted that the hot extrusion scheme predicted very close to experimental results when a correction factor was applied. Zolfaghari et al. (2010) also stated that plastic plug flow of wood-plastic composite was observed in the die. In this study, the pressure distribution along the briquetting die is investigated assuming plug flow through the die with an adaptation of the hot extrusion scheme.

2 Development of mathematical model

Following the study of Zolfaghari et al. (2010) and Behravesh et al. (2010), a plastic plug flow behaviour of compacted biomass through the die entry and the briquetting die is assumed. It is also assumed that Coulomb frictional condition exists at the interface between compacted biomass and the die; slipping occurs at the boundary of the material and the die; the coefficients of friction are independent of pressure or temperature; pressures within the plug are non-isotropic; and strain-hardening effect on the biomass material is neglected. These assumptions are used to develop pressure distribution models along the die entry and the briquetting die. The geometry of the extrusion die being considered is shown in the schematic diagram in Figure 1.

Figure 1 Schematic illustration of the extrusion die geometry for the screw extruder briquetting machine

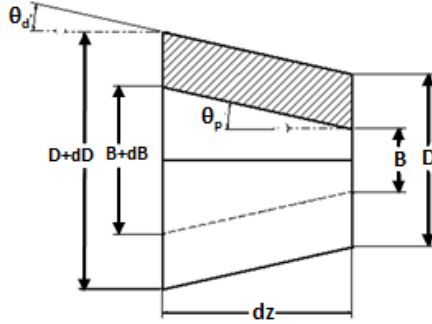


2.1 Pressure distribution along the conical die entry

The die entry is a conical frustum with a taper angle of θ_p . An elemental slice of material flowing through the die entry is considered. Figure 2 shows the dimensions of an elemental slice of plug of the material flowing through the die entry. The material flowing has a hole made in it by the design of the screw which is also important to facilitate the burning of the briquette. The taper angle of the die is θ_d while the taper

angle of the end of screw making the hole is θ_p . The hole diameter is in terms of B while the diameter at the interface between compacted material and the die is in terms of D .

Figure 2 Schematic diagram of an elemental slice of plug flowing through the conical die entry of the biomass briquetting machine



2.1.1 Frictionless die pressure distribution along the conical die entry

Behravesh et al. (2010) stated that for composites with highly filled solid (wood) component, the flow behaviour in the die is closer to the hot extrusion scheme. From the hot extrusion scheme, the ideal pressure is the extrusion pressure when friction is neglected. Therefore, the minimum extrusion pressure of biomass through the conical entry is modelled by assuming that the extrusion is frictionless. Hence, the work done per unit volume can be expressed as (Dieter, 1988):

$$\frac{W}{V} = \int \sigma d\epsilon \quad (1)$$

By assuming that the stress, σ , equals the yield strength, Y , of the compacted biomass material, equation (1) can be written as:

$$\frac{W}{V} = \int Y d\epsilon = Y \int d\epsilon \quad (2)$$

The strain can be written as $d\epsilon = \frac{dl}{l}$ such that the work done per unit volume is expressed as:

$$\frac{W}{V} = Y \int \frac{dl}{l} = Y \ln \int \frac{l_2}{l_1} \quad (3)$$

From Equation (3), l_1 and l_2 represent, respectively, the lengths of the biomass compact before and after passing through the die entry. Constancy of volume ($A_1 l_1 = A_2 l_2$) is

assumed such that $\frac{l_2}{l_1} = \frac{A_1}{A_2}$. This is substituted into equation (3) so that it can be written as:

$$\frac{W}{V} = Y \ln \frac{A_1}{A_2} \quad (4)$$

Work done can be expressed as a product of the pressure and volume, such that:

$$W = P_{d1}V \quad (5)$$

Therefore, from equation (4) and equation (5), the die pressure for frictionless extrusion is:

$$P_{d1} = Y \ln \frac{A_1}{A_2} \quad (6)$$

Mulji and Mackley (2003) and Horrobin and Nedderman (1998) stated that a model similar to equation (6) can be used as lower bound for pressure difference across the die entry. Behravesh et al. (2010) opined that there is a need to modify the yield strength with a correction coefficient which is considered as a function of material compaction. The correction factor takes into consideration the strong dependence of tensile strength on temperature in the model. Taking the correction coefficient as ζ , and writing equation (6) in terms of the diameters at the start and end of the die entry:

$$P_{d1} = \zeta Y \ln \left[\frac{D_1^2 - B_1^2}{D_2^2 - B_2^2} \right] \quad (7)$$

The angle of the die entry can be written in terms of the entry and exit diameters, D_1 and D_2 , and the length, L_r , of the conical die entry. The angle of the end of the screw making the central hole in the briquette can be written in terms of the diameters, B_1 and B_2 and the length L_r . These are given as:

$$\tan \theta_d = \frac{D_1 - D_2}{2L_r}; \quad \tan \theta_p = \frac{B_1 - B_2}{2L_r} \quad (8)$$

The annular ratio of the die, which is the ratio of the diameter of the central hole to the diameter of the briquette, B_2/D_2 , is represented by ζ . The frictionless die pressure can then be written as:

$$P_{d1} = \zeta Y \ln \left\{ 1 + \frac{2L_r (\tan \theta_d - \zeta \tan \theta_p)}{D_2 (1 - \zeta^2)} + \frac{4L_r (\tan^2 \theta_d - \tan^2 \theta_p)}{D_2^2 (1 - \zeta^2)} \right\} \quad (9)$$

The pressure distribution along the length of the die in the z-direction can then be written as:

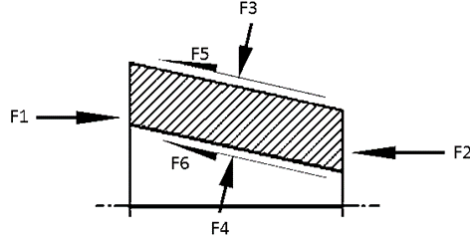
$$P_{dz} = \zeta Y \ln \left\{ 1 + \frac{2(L_r - z) \cdot (\tan \theta_d - \zeta \tan \theta_p)}{D_2 (1 - \zeta^2)} + \frac{4(L_r - z) \cdot (\tan^2 \theta_d - \tan^2 \theta_p)}{D_2^2 (1 - \zeta^2)} \right\} \quad (10)$$

Equation (10) shows that the model for frictionless die entry pressure for the conical die entry reduces along the length of the die and is zero at the end of the conical die entry, where $z = L_r$.

2.1.2 Frictional pressure distribution along the conical die entry

In addition to the ideal pressure, the pressure required to overcome the friction needs to be considered to fully describe the pressure distribution at the die. Figure 3 shows the forces acting on the elemental slice of the plug of material flowing through the die entry. F_1 and F_2 are due to the uniaxial pressure exerted on the compacted biomass material. F_3 and F_4 are lateral pressures due to stress transmission of the uniaxial pressure. F_5 is the frictional force at the interface between the compacted material and the die. F_6 is the frictional force at the interface between the compacted material and the end of the screw making the hole.

Figure 3 Forces acting on the elemental slice of material flowing through the conical die entry



A force analysis is carried out on the elemental slice of the plug to obtain a mathematical model for the pressure along the conical entry of the die. The force, F_1 , due to the uniaxial pressure on the surface of the plug is expressed as:

$$F_1 = P \frac{\pi}{4} [(D + dD)^2 - (B + dB)^2] \quad (11)$$

The force F_2 , being the resisting pressure at the end of the plug in opposite direction to F_1 , is expressed as:

$$F_2 = (P + dp) \frac{\pi}{4} [(D^2 - B^2)] \quad (12)$$

The force F_3 is due to the pressure transmission and acts on the die wall. Force F_3 is, therefore, expressed as:

$$F_3 = \kappa P \frac{\pi}{2} (2D + dD) dz \quad (13)$$

The lateral stress coefficient, or stress transmission coefficient, κ , is defined in terms of the effective angle of powder friction, ϕ_e , as (Ennis et al, 2008):

$$\kappa = \frac{1 - \sin \phi_e}{1 + \sin \phi_e} \quad (14)$$

The force F_4 is also due to stress, or pressure, transmission but acts on the surface of the screw which creates the hole at the centre of the briquette. Force F_4 is expressed as:

$$F_4 = \kappa P \frac{\pi}{2} (2B + dB) dz \quad (15)$$

Force F_5 is a frictional force due to the normal force F_3 acting on the surface of the die and is expressed as:

$$F_5 = \mu_d F_3 = \mu_d \kappa P \frac{\pi}{2} (2D + dD) dz \quad (16)$$

Force F_6 is also a frictional force but acts on the surface of the screw. Force F_6 is expressed as:

$$F_6 = \mu_s F_4 = \mu_s \kappa P \frac{\pi}{2} (2B + dB) dz \quad (17)$$

The force balance on the element, along the z-direction is:

$$F_1 - F_2 - F_3 \sin \theta_d + F_4 \sin \theta_p - F_5 \cos \theta_d - F_6 \cos \theta_p = 0 \quad (18)$$

Equations (11) to (17) are substituted into equation (18). After simplification of the equation by neglecting products and multiples of infinitesimal terms, the force balance is written as:

$$\begin{aligned} PD \frac{dD}{2} - PB \frac{dB}{2} - D^2 \frac{dP}{4} + B^2 \frac{dP}{4} - \kappa PDz \sin \theta_d + \kappa PBdz \sin \theta_p \\ - \mu_d \kappa PDdz \cos \theta_d - \mu_s \kappa PBdz \cos \theta_p = 0 \end{aligned} \quad (19)$$

From the geometry in Figure 2, dB can be expressed in terms of dz as:

$$dB = 2dz \tan \theta_d \quad (20)$$

Also, dD can be expressed in terms of dz as:

$$dD = 2dz \tan \theta_d \quad (21)$$

Also, taking the annular ratio of the die as ζ_z at any given section, the diameter screw end making the hole at the centre of the briquette can be expressed in terms of the diameter of the die as $B = \zeta_z D$. In terms of the distance along the die, the annular ratio at any given section is expressed as:

$$\zeta_z = \frac{B_1 - 2z \tan \theta_p}{D_1 - 2z \tan \theta_d} = \frac{\zeta D_2 + 2(L_t - z) \tan \theta_p}{D_2 + 2(L_t - z) \tan \theta_d} \quad (22)$$

By substituting equation (20) to (22) into equation (19) and simplifying, the expression becomes:

$$\frac{dP}{P} = \frac{4}{D} \left\{ \frac{\left[\begin{aligned} &(\tan \theta_d - \kappa \sin \theta_d - \mu_d \kappa \cos \theta_d) \\ &-\zeta_z (\tan \theta_p - \kappa \sin \theta_p - \mu_d \kappa \cos \theta_p) \end{aligned} \right]}{(1 - \zeta_z^2)} \right\} dz \quad (23)$$

Equation (22) can be integrated taking the initial condition at the beginning of the conical die entry as:

$$z = 0; P - P_{\max} - P_{d1} \quad (24)$$

P_{\max} is the total die pressure at the end of the screw extruder just before the die entry. By integrating equation (23) with the condition stated in equation (24):

$$\ln \frac{P}{(P_{\max} - P_{d1})} = \frac{4z}{D} \left\{ \frac{\left[\frac{(\tan \theta_d - \kappa \sin \theta_d - \mu_d \kappa \cos \theta_d)}{(1 - \zeta_z^2)} \right]}{-\zeta_z (\tan \theta_p - \kappa \sin \theta_p - \mu_s \kappa \cos \theta_p)} \right\} \quad (25)$$

The mathematical model for the pressure distribution along the length of the die is therefore:

$$P_z = (P_{\max} - P_{d1}) \exp \left\{ \frac{4z}{D} \left[\frac{\left[\frac{(\tan \theta_d - \kappa \sin \theta_d - \mu_d \kappa \cos \theta_d)}{(1 - \zeta_z^2)} \right]}{-\zeta_z (\tan \theta_p - \kappa \sin \theta_p - \mu_s \kappa \cos \theta_p)} \right] \right\} \quad (26)$$

Equation (26) shows the pressure variation along the length of the die in the z-direction.

2.2 Frictional pressure distribution along the briquetting die

The briquetting die also contributes to the pressure required for extrusion of compacted biomass materials. The briquetting die is the cylindrical part of the die which is positioned after the conical die entry and shown by length L_d in Figure 1. For the analysis, the geometry of an element of the plug of material flowing through the briquetting die is shown in Figure 4. The forces acting on the plug are shown in Figure 5.

Figure 4 Geometry of plug flowing through the briquetting die

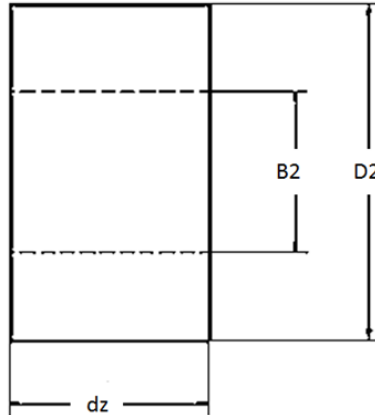
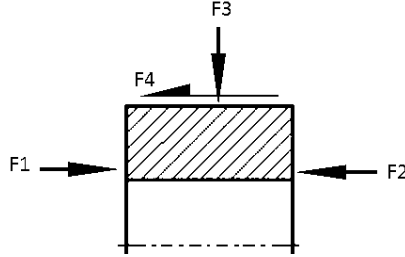


Figure 5 Forces acting on the plug of material flowing through the briquetting die



The force $F1$ is the force due to the exerted pressure at the side closer to the die entry and it is expressed as:

$$F1 = P \frac{\pi}{4} (D^2 - B^2) \tag{27}$$

Force $F2$ is the force which acts opposite to the pushing force $F1$ and is expressed as:

$$F2 = (P + dP) \frac{\pi}{4} (D^2 - B^2) \tag{28}$$

Force $F3$ is due to stress transmission and is expressed as:

$$F3 = \kappa P \pi D dz \tag{29}$$

Force $F4$ is a frictional force and is expressed as:

$$F4 = \mu_d F3 = \mu_d \kappa P \pi D dz \tag{30}$$

A force balance is taken over the element in the direction of the flow, which is the z -direction. The force balance over the element is:

$$F1 - F2 - F4 = 0 \tag{31}$$

By substituting equation (27) to (30) into equation (31) and simplifying, the expression for the force balance is:

$$\frac{dP}{P} = - \frac{4\mu_d \kappa D}{D^2 - B^2} dz \tag{32}$$

Equation (32) is integrated by taking the initial condition as the pressure at the beginning of the briquetting die, which is equal to the pressure at the end of the conical die entry, expressed as:

$$z = 0; P = (P_{\max} - P_{d1}) \exp \left\{ \frac{4L_d}{D} \left[\frac{(\tan \theta_d - \kappa \sin \theta_d - \mu_d \kappa \cos \theta_d)}{(1 - \zeta^2)} \right] \right\} \tag{33}$$

The pressure gradient, or distribution, along the length of the die is therefore expressed as:

$$\ln \frac{P_z}{P_o} = -\frac{4\mu_d \kappa D z}{D^2 - B^2} \quad (34)$$

Equation (34) can be written in exponential form as:

$$P_z (P_{\max} - P_{d1}) \cdot \exp \left[\frac{4L_d}{D_2} \left\{ \frac{(\tan \theta_d - \kappa \sin \theta_d - \mu_d \kappa \cos \theta_d)}{-\zeta (\tan \theta_p - \kappa \sin \theta_p - \mu_s \kappa \cos \theta_p)} \right\} - \frac{4\mu_d \kappa z}{D_2 (1 - \zeta^2)} \right] \quad (35)$$

Equation (35) is the mathematical model for the pressure variation along the length of the briquetting die with the pressure at the beginning of the briquetting die being the pressure at the end of the conical die entry. As it had been observed, the frictionless die pressure diminishes to zero at the beginning of the briquetting die.

3 Results and discussion

The parameters utilised in simulation of the pressure developed along the die entry and briquetting die are presented in Table 1.

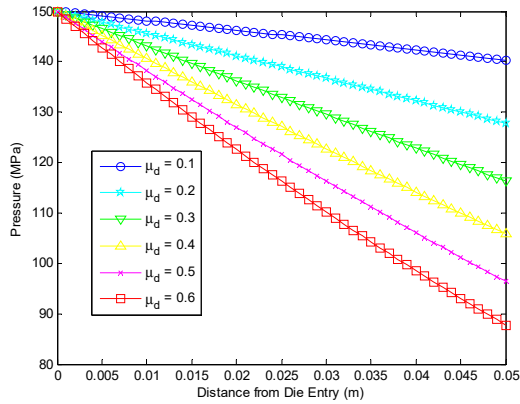
Table 1 Parameters for the simulation of the extrusion die of a screw extruder briquetting machine

| Parameter | Symbol | Value |
|-------------------------------------|------------|---------------|
| Maximum pressure | P_{\max} | 150 MPa |
| Diameter of briquetting die | D | 60 mm |
| Die entry angle | θ_D | 2.45°, varied |
| Die annular ratio | ζ | 0.5 |
| Yield strength of compacted biomass | Y | 50 – 100 MPa |
| Correction factor | ξ | 0.5 |

3.1 Effect of friction coefficient on the pressure distribution along the die entry

The effect of friction coefficient at the die on the pressure along the length of the die entry is shown in Figure 6. The figure shows that as the briquetting die is approached from the entry into the die region, there is a decrease in the pressure at sections along the axial length of the die towards the die exit. Similar observations have been made by Križan et al. (2012) and Kováčová et al. (2014). It is also observed from Figure 6 that the friction coefficient at the interface between the die and compacted biomass has effects on the pressure at different sections along the die entry. The pressure at different positions is lower with an increased frictional coefficient at the interface between the compacted biomass and the die. Similar observations have been discussed by Kováčová et al. (2014) although their study had not included the effect of yield strength of biomass included in the ideal extrusion pressure. It may also be deduced from Figure 6 that the die pressure will be higher when the friction coefficient between the biomass compact and the die is increased.

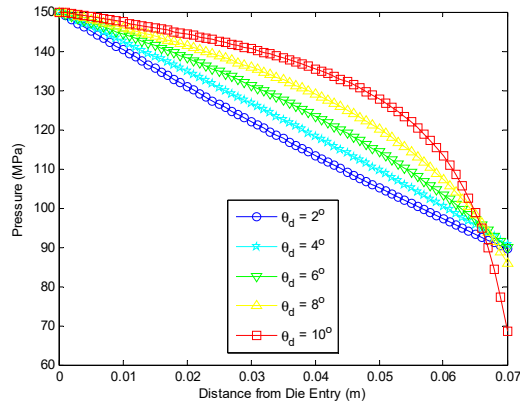
Figure 6 Effect of friction coefficient at the die on the pressure distribution along the tapered die entry (see online version for colours)



3.2 Effect of die entry angle on the pressure distribution along the die entry

The effect of the die entry angle on the pressure along the position of the die is shown in Figure 7. As observed, the pressure at different sections of the die decreases towards the outlet but an increase on the die entry angle causes a slower drop in the pressure at the various positions. Figure 7 also shows that higher die taper angles have curves with convex shapes which reverses the effects when the die length considered is much longer than the specified range. This implies that there has to be a die angle which will give a minimum extrusion pressure required for the screw briquetting machine.

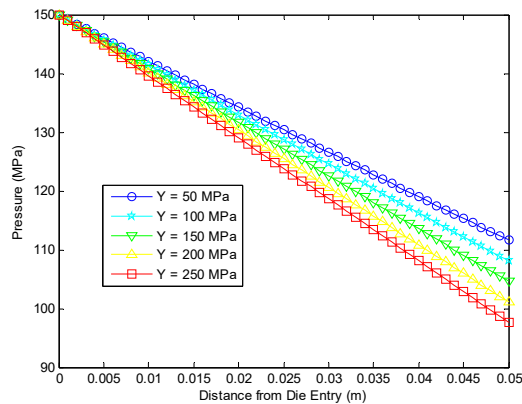
Figure 7 Effect of the die entry angle on the pressure distribution at the tapered die entry (see online version for colours)



3.3 Effect of yield strength on the pressure distribution along the die entry

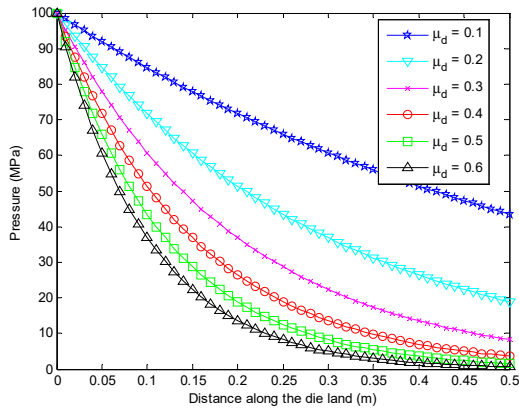
The effect the yield strength of the compacted biomass materials on the pressure distribution along the die entry is shown in Figure 8. It is observed that the higher the yield strength of the compacted biomass material, the faster the pressure will drop along the die entry. The implication of this is that the property of the biomass material being processed through the die influences the pressure along the die entry. Also, biomass compact with higher yield strength will result in higher die pressure at the end of the screw extruder.

Figure 8 Effect of yield strength on the pressure distribution at the briquetting die (see online version for colours)



3.4 Effect of friction coefficient on the pressure distribution along the briquetting die

The effect of friction coefficient on the pressure distribution along the axial length of the briquetting die is shown in Figure 9. The pressure is seen to drop at different sections along the axial length of the briquetting die as the compacted biomass approaches the exit of the die. It is also observed that when a smaller friction coefficient exists at the interface between the compacted biomass and the walls of the briquetting die, the pressure decreases gradually. However, the pressure decreases quite rapidly as the friction coefficient at the interface is increased. As pointed out for the die entry, the die pressure at the end of the screw extruder will be higher when the friction coefficient at the interface between the biomass compact and the briquetting die is increased.

Figure 9 Effect of friction coefficient on the pressure distribution at the briquetting die (see online version for colours)

4 Conclusions

The pressure distribution along the extrusion die has been modelled in this study. The model for the die entry considers the ideal die pressure and the frictional die pressure whilst the briquetting die requires only the consideration of frictional pressure. The pressure distribution along the die entry is affected by the yielding property of the biomass material, the die angle and the friction coefficient at the die interface. Increased friction coefficient and high yield strength of biomass compacts resulted in rapid pressure decrease in the briquetting die, and consequently, result in higher die pressure at the end of the screw extruder. The study also showed that the effect of the die angle along the length of the briquetting die varied depending on the length of the die entry. Pressure distribution of the briquetting die with specified geometry decreased with increase in friction coefficient at the interface of the compacted biomass and the briquetting die. The results from this study could have significant impact on the design of screw extruder briquetting machines.

References

- Behraves A.H., Shakouri, E., Zolfaghari, A. and Golzar, M. (2010) 'Theoretical and experimental study on die pressure prediction in extrusion of wood-plastic composite', *Journal of Composite Materials*, Vol. 44, No. 11, pp.1293–1304.
- Dieter, G.E. (1988) *Mechanical Metallurgy*, McGraw Hill, London.
- Ennis, B.J., Witt, W., Sphar, D., Gommeran, E., Snow, R.H., Raymus, G.J. and Litster, J.D. (2008) 'Solid-solid operations and processing', Section 21, In *Perry's Chemical Engineering Handbook*, 8th ed., McGraw-Hill Companies, USA.
- Hardman, J.S. (2001) *Briquetting of Rice Husk and Production of Value-Added Products from Rice Husk*, Progress Report of DFID Project – R7659: Benefits of Improved Rice Husk Combustion Efficiency, pp.3–6.

- Horrobin, D.J. and Nedderman, R.M. (1998) 'Die entry pressure drops in paste extrusion', *Chemical Engineering Science*, Vol. 53, No. 18, pp.3215–3225.
- Jarošová, E. and Kureková, E. (2013) 'Determination of optimal technological parameters of a compaction process: case study', *Measurement Science Review*, Vol. 13, No. 1, pp.12–19.
- Kováčová, M., Matúš, M., Križan, P. and Beniák, J. (2014) 'Design theory for the pressing chamber in the solid biofuel production process', *Acta Polytechnica*, Vol. 54, No. 1, pp.28–34.
- Križan, P., Matúš, M. and Šooš, L. (2012) 'Design of pressing chamber of briquetting machine with horizontal pressing axis', *Proceedings of 11th International Scientific Conference: Advanced Production Technologies*, Novi Sad, Serbia, 20–21 September.
- Križan, P., Šooš, L. and Matúš, M. (2010) 'Optimisation of briquetting machine pressing chamber geometry', *Machine Design*, ISSN 1821-1259:19-24.
- Križan, P., Šooš, L. and Vukelic, Dj. (2009) 'Counter pressure effecting on compacted briquette in pressing chamber', *Journal of Production Engineering*, Vol. 12, No. 1, pp.63–66.
- Kumararaja, L. (2009) *Development of Gasifier Suitable for Non-Woody Bioresidues for Electric Power Generation*, Project report, Department of Science, Technology and Environment, Govt. of Puducherry, Puducherry – 605-014.
- Manickam, I.N., Suresh, S.R. (2011). 'Densification characteristics of coir pith', *International Journal of Engineering Science and Technology*, Vol. 3, No. 4, pp.2590–2595.
- Matúš, M., Križan, P., Ondruška, J. and Šooš, L. (2011) 'Analysis of tool geometry for screw extrusion machines', *Journal of Applied Mathematics*, Vol. 6, No. 2, pp.404–414.
- Maurya, R.K., Patel, A.R., Sarkar, P., Singh, H. and Tyagi, H. (2018) 'Biomass, its potential and applications', in Kumar, S. and Sani, R. (Eds.): *Biorefining of Biomass to Biofuels. Biofuel and Biorefinery Technologies*, Vol. 4, pp.25–52, Springer, Cham.
- Mulji, N.C. and Mackley, M.R. (2003) 'The axisymmetric extrusion of solid chocolate and the effect of die geometry', *International Journal of Forming Processes*, Vol. 6, No. 2, pp.161–178.
- Ojolo, S.J. and Orisaleye, J. I. (2010) 'Design and development of a laboratory scale biomass gasifier', *Journal of Energy and Power Engineering*, August, Vol. 4, No. 8, pp.16–23.
- Ojolo, S.J., Ajiboye, J.S. and Orisaleye, J.I. (2015) 'Plug flow analysis for the design of the compaction region of a tapered screw extruder biomass briquetting machine', *Agric. Eng. Int.: CIGR Journal*, Vol. 17, No. 3, pp.176–195.
- Ojolo, S.J., Orisaleye, J.I., Ismail, S.O. and Abolarin, S.M. (2012a) 'Technical potential of biomass energy in Nigeria', *Ife Journal of Technology*, Vol. 21, No. 2, pp.60–65.
- Ojolo, S.J., Orisaleye, J.I., Ismail, S.O. and Odutayo, A.F. (2012b) 'Development of an inverted downdraft biomass gasifier', *Journal of Emerging Trends in Engineering and Applied Sciences*, Vol. 3, No. 3, pp.513–516.
- Orisaleye, J.I. and Ojolo, S.J. (2019) 'Parametric analysis and design of straight screw extruder for solids compaction', *Journal of King Saud University – Engineering Sciences*, Vol. 31, No. 1, pp.86–96.
- Orisaleye, J.I., Ojolo, S.J. and Ajiboye, J.S. (2019) 'Pressure build-up and wear analysis of tapered screw extruder biomass briquetting machines', *Agricultural Engineering International: CIGR Journal*, Vol. 21, No. 1, pp.122–133.
- Smeets, E., Faaji, A. and Lewandoski, I. (2014) *A Quick Scan of Global Bio-Energy Potentials to 2050 – An Analysis of the Regional Availability of Biomass Resources for Export in Relation to Underlying Factors*, Report prepared for NOVEM and Essent, Copernicus Institute – Utrecht University, NWS-E-2004-109, March 2004.
- Tumuluru, J.S., Wright, C.T., Kenny, K.L. and Hess, J.R. (2010) *A Review on Biomass Densification Technologies for Energy Application*, Idaho National Laboratory, U.S. Department of Energy, IN/EXT-10-18420, August.
- Zhong, Z. (1991) *Theoretical and Experimental Analysis of the Compaction Process in a Tapered Screw Press*, Doctor of Philosophy thesis, The University of Newcastle upon Tyne.

Zolfaghari, A., Behravec, A.H., Shakouri, E. and Soury, E. (2010) 'Flow balancing in die design of wood flour/HDPE composite extrusion profiles with consideration of rheological effect', *Polymer Engineering and Science*, Vol. 50, No. 3, pp.543–549.

Notations

| | |
|------------------------|--|
| A_1 | Cross sectional area of compact before passing through die entry |
| A_2 | Cross sectional area of compact after passing through die entry |
| B | Diameter of hole in compacted material |
| B_1 | Diameter of hole at the inlet of die entry |
| B_2 | Diameter of hole at exit of die entry |
| D | Diameter of compacted material |
| D_1 | Inlet diameter of die entry |
| D_2 | Diameter of briquetting die / exit diameter of die entry |
| F_1, F_2, \dots, F_6 | Forces acting on elemental slice |
| L_d | Length of briquetting die |
| L_t | Length of die entry |
| l_1 | Length of compacted material before passing through die entry |
| L_2 | Length of compacted material after passing through die entry |
| P | Pressure |
| P_{d1} | Frictionless die pressure |
| P_{dz} | Frictionless pressure along the die entry |
| P_{fx} | Frictional pressure along the die entry |
| P_z | Pressure along the briquetting die |
| P_{max} | Maximum pressure at the die entry |
| V | Volume |
| W | Work done |
| Y | Yield strength |
| ϵ | Strain |
| ζ | Annular ratio of the briquetting die |
| ζ_c | Annular ratio of the die entry |
| θ_d | Taper angle of the die entry |
| θ_p | Taper angle of screw end |
| κ | Stress transmission coefficient |
| μ_d | Friction coefficient at the die interface |
| M_s | Friction coefficient at the screw end |
| σ | Stress |
| χ | Correction factor |
